BIOLOGY OF REPRODUCTION **60,** 580–587 (1999)

Differential Transcriptional Activity Associated with Chromatin Configuration in Fully Grown Mouse Germinal Vesicle Oocytes[1]

Christine Bouniol-Baly,[4] Lahcen Hamraoui,[3,6] Juliette Guibert,[4] Nathalie Beaujean,[4] Maria S. Szöllösi,[4] and Pascale Debey[2,4,5]

Laboratoire INRA (806),[4] Institut de Biologie Physico-Chimique, 75005 Paris, France
Muséum National d'Histoire Naturelle,[5] 75005 Paris, France
Laboratoire de Biochimie appliquée,[6] Université Chouaib Doukhali, El Jadida, Morocco

ABSTRACT

It was previously shown that fully grown ovarian germinal vesicle (GV) oocytes of adult mice exhibit several nuclear configurations that differ essentially by the presence or absence of a ring of condensed chromatin around the nucleolus. These configurations have been termed, respectively, SN (surrounded nucleolus) and NSN (nonsurrounded nucleolus). Work from our and other laboratories has revealed ultrastructural and functional differences between these two configurations. The aims of the present study were 1) to analyze the equilibrium between the SN and the NSN population as a function of the age of the mice and the time after hCG-induced ovulation and 2) to study the polymerase I (pol I)- and polymerase II (pol II)-dependent transcription in both types of oocytes through the detection of bromouridine incorporated into nascent RNA. We show 1) that ovarian GV oocytes exhibiting the SN-type configuration can be found as soon as 17 days after birth in the C57/CBA mouse strain and 2) that the SN:NSN ratio of ovarian GV oocytes is very low just after hCG-induced ovulation and then increases progressively with the time after ovulation.

Furthermore, we demonstrate that the SN configuration correlates strictly with the arrest of both pol I- and pol II-dependent transcription in mice at any age. Finally, we show that ribosomal genes are located at the outer periphery of the nucleolus in the NSN configuration and that pol I-dependent perinucleolar transcription sites correspond to specific ultrastructural features of the nucleolus.

Altogether, these results provide clear-cut criteria delineating transcriptionally active GV oocytes from those that are inactive, and confirm that the SN-type configuration is mostly present in preovulatory oocytes.

INTRODUCTION

Clearly characterizing preovulatory oocytes biochemically and morphologically, as well as obtaining criteria for the quality of oocytes—i.e., their capacity to resume and complete meiosis but also to sustain complete embryonic development after fertilization—is of prime importance in mammalian reproduction owing to the increased use of in vitro maturation/fertilization protocols. Data obtained in several mammals [1–3] show that the size of follicles and oocytes represents a primary essential parameter. However, more subtle biochemical changes are likely to be associated with the last step toward ovulation. In the mouse, for example, it has previously been shown that fully grown oocytes do not present a homogeneous chromatin pattern [4–7]. Germinal vesicle (GV)-stage oocytes from large antral follicles can actually be grouped into two distinct major classes. In the first class, termed SN (surrounded nucleolus), chromatin is rather condensed and is particularly confined around the 'nucleolus-like body'' (NLB; this term will be used [8, 9] instead of 'nucleolus'' because of the unusual ultrastructure and function of this nuclear compartment in fully grown GV oocytes). In the second class, termed NSN (nonsurrounded nucleolus), chromatin is less condensed and does not surround the NLB. Intermediate configurations include one with aggregates of condensed chromatin apposed to the NLB (partly NSN) and one with a partial perinucleolar chromatin ring (partly SN).

Several observations suggest that the SN configuration represents a stage of GV oocyte that is more advanced toward ovulation: 1) the fact that only the NSN configuration is found in preantral follicles [4, 6] and that the SN configuration arises only around the 18th day after birth [5]; 2) the smaller size of NSN oocytes [5–7]; 3) their lower in vitro-maturation speed and rate [6]; 4) the more pronounced M-phase characteristics of SN oocytes in terms of microtubule array and phosphoprotein content [5]; and 5) the recent finding of their higher rate of development to 4-cells after in vitro maturation and fertilization [10]. A similar perinucleolar chromatin ring has been described in other species, such as the rat [11], pig [12], monkey [13], and human [14, 15], and, in the latter case, was shown to characterize the preovulatory stage. However, the facts that 1) NSN oocytes mature in vitro without previous transformation into the SN configuration [6] and 2) are able to develop beyond the 2-cell stage, although to a lesser extent, after in vitro maturation and fertilization [10], to some extent contradict this hypothesis. Moreover, the possibility that the mouse SN and the human SN-like configurations could represent a step toward atresia has been envisioned [7, 15], as 66% of the configuration with condensed perinucleolar chromatin is atretic in monkeys [13].

Parallel to the structural characterization of preovulatory GV oocytes, their transcriptional status is still a matter of debate. Moore et al. [16] reported a complete cessation of all transcriptional activities in mouse oocytes from large antral follicles, while others found [^{3}H]uridine incorporation in mouse GV preovulatory oocytes [9, 17–19] even up to 2 h before GV breakdown (GVBD) [18, 19]. In other mammals, such as cattle [3, 20], pigs [12, 21], and sheep [22], a dramatic decrease in polymerase II (pol II)-dependent heterogenous nuclear RNA (hnRNA) synthesis has been observed as the antrum grows (for review see [22]). Continuing RNA synthesis was observed in human GV oo-

Accepted October 6, 1998.
Received May 21, 1998.
[1]This work was financially supported by the Institut National de la Recherche Médicale (INSERM) and Institut National de la Recherche Agronomique (INRA).
[2]Correspondence: Pascale Debey, Laboratoire INRA (806), Institut de Biologie Physico-Chimique, 13 rue P. et M. Curie, 75005 Paris, France. FAX: 33 1 43 29 80 88; e-mail: debey@ibpc.fr
[3]Current address: Laboratoire de Biologie marine, Université P. et M. Curie, CNRS UPR 9042, 7 quai St. Bernard, 75005 Paris, France.

cytes recovered from preovulatory follicles [8, 14] but not in those from nonovulatory follicles [23], while subsequent studies showed a direct link between the presence of a characteristic chromatin mass around the NLB (called ''karyosphere'') and transcriptional inactivity [15]. Similarly, polymerase I (pol I)-dependent [^{3}H]uridine incorporation into rRNAs was shown to decrease dramatically and to become essentially restricted to the nucleolar periphery at the end of the ovarian growth phase, i.e., when the electron-dense nucleolar area develops [12, 14, 20, 22]. Our previous ultrastructural analyses suggested a residual transcriptional activity of ribosomal genes in NSN-type NLB [6], while the distribution of the splicing factor SC35 was consistent with a lower hnRNA synthesis activity in the SN-type configuration [24]. Therefore it is still not clear whether complete transcriptional activity cessation characterizes the preovulatory stage of GV oocytes.

With reference to these studies, we decided to further analyze 1) the time dependence of the SN:NSN ratio in GV oocytes from antral follicles in adult mice after hormonal stimulation of ovulation and 2) the relationship between chromatin configuration and pol I- and pol II-dependent RNA synthesis activity.

MATERIALS AND METHODS

Collection and Culture of Oocytes

Ovarian GV oocyte-cumulus complexes were collected from juvenile (15 to 21 days old) and adult (28 days to several weeks old) C57/CBA mice by random puncture of the ovary, as previously described [25]. Compact complexes in which the cumulus cell layer(s) could not be mechanically separated from the oocytes were discarded. The others, which represent oocyte-cumulus complexes from antral follicles, were gently pipetted through a mouth glass pipette to remove most cumulus cells. Oocytes were then cultured in modified culture medium M2 (4.15 mM sodium bicarbonate, 20.85 mM Hepes, 4 mg/ml BSA) at 37°C according to standard procedures. The age of the mice was known with an accuracy of 12 h. Oocytes from adult mice were all of diameter > 70 μm (i.e., from antral follicles). The size of oocytes collected from juvenile mice was not checked.

Stimulation of Ovulation

The distribution of GV oocytes presenting the various chromatin configurations was analyzed at different times after ovulation. For that purpose, ovulation was stimulated in 12–20 mice through an i.p. injection of 5 IU hCG (Intervet, Angers, France). Several such synchronized mice were killed at each time point, and oocytes were collected as described above. For time points between 13 and 24 h post-hCG injection (time phCG), only mice in which ovulation could be assessed by the presence of ovulated oocytes in the ampullae were included in the study. For other time points, mice from which too small a number of ovarian oocytes had been collected were excluded. Three independent experiments were done, two with young (28 days old) and one with older (6 to 8 wk old) mice. At each time point, the SN:NSN ratio (R) was measured for each mouse, and the mean and SD values were calculated. As the number of R values at each time point was very low (1–5), the significance of the differences from point to point was assessed by the Wilcoxon-Mann-Whitney (WMW) test.

In one experiment, ovarian stimulation was performed with an i.p. injection of 5 IU of eCG (Intervet) 24 h after hCG injection.

Hoechst Labeling for Assessment of the Chromatin Configuration in Live or Fixed Oocytes

Methods employed were those from Debey et al. [6]. GV oocytes were labeled by addition of 5 ng/ml (8 nM) of Hoechst 33342 (Riedel-deHaën, Germany) to the culture medium starting from the puncture of ovaries. They were then distributed individually in small droplets of medium containing the same concentration of Hoechst in Petriperm dishes (Bachofer GmbH, Reutlingen, Germany) under paraffin oil (BdH Laboratory Supplies, Poole, England). Observations were performed with a Zeiss (Carl Zeiss, Thornwood, NY) inverted microscope equipped with an intensified camera (Lhesa, Cergy Pointoise, France) coupled to an image digitalization and analysis system (Quantel Microconsultants, Montigny le Bretonneux, France). Hoechst fluorescence was obtained by excitation at 360 nm using a mercury lamp (50 W) attenuated 100 times with neutral filters. Duration of the observations did not exceed 5 sec. These conditions have been shown not to cause major impairment of oocyte viability [6]. Classification of oocytes was done according to Debey et al. [6] in four groups: NSN, SN, pNSN (partly NSN, i.e., with 3–4 heterochromatin granules apposed to the NLB), and pSN (partly SN, i.e., with heterochromatin partly wrapped around the NLB).

When observation of live oocytes was not required, collected oocytes were fixed in 2% paraformaldehyde (PFA; Merck, Rahway, NJ) in PBS for 20 min at room temperature, rinsed in PBS, and labeled by addition of 2 μg/ml Hoechst 33342 to the PBS for 20 min. Observations were performed as described for live oocytes. Statistical significance of the differences in percentage of NSN-, pSN-, and SN-type oocytes was assessed by chi-square analysis.

Oocyte size was measured on digitalized images using the image analysis system, the significance of the differences between SN and NSN types being analyzed by the chi test.

Fluorescent Detection of pol I- and pol II-Dependent Transcriptional Activities

Oocytes were collected and handled in M2 containing 100 μg/ml dibutyryl cAMP (dbcAMP; Sigma Chemical Co., St. Louis, MO) to prevent resumption of meiosis. Transcription was assayed through immunofluorescent detection of bromouridine (BrU) incorporated into nascent RNAs, according to a method previously developed for somatic cells [26] and adapted to mouse embryos [27]. Bromo-UTP (Br)UTP (Sigma; 100 mM in 2 mM Pipes [pH 7.5] + 140 mM KCl) was introduced through microinjection into the cytoplasm of oocytes. After a 10- to 30-min culture in M2+dbcAMP, oocytes were rinsed, fixed in 2% PFA in PBS for 20 min at room temperature, and permeabilized for 15 min by 0.2% Triton X-100 in PBS before being processed for immunodetection of incorporated BrU as described below. To detect exclusively pol I transcription sites, oocytes were first incubated for 1 h in M2+dbcAMP containing 10 μg/ml α-amanitin (Sigma). They were then microinjected with BrUTP as above, except that α-amanitin (50 μg/ml) was added to the microinjection solution. These conditions had been previously shown to ensure the proper inhibition of pol II but not pol I [27]. Oocytes were then cultured for 10–30 min in M2+dbcAMP before being rinsed, fixed, and permeabilized as described above. To in-

TABLE 1. Repartition of ovarian GV oocytes in juvenile mice as a function of the age of the mice.

Age of mice (days)	No. of mice	Total no. oocytes	NSN+PSN		pSN		SN		
			No.	%	No.	%	No.		%
15	2	59	57[a]	96.6	2[b]	0.4		0	
16	2	41	37[a]	90.0	4[b]	10.0		0	
17	4	139	112[c]	80.6	12[e]	8.6	15[f]		10.8
18	2	121	74[d]	61.0	27[e]	22.3	20[f]		16.6

[a–f] Within a column, numbers with the same superscript are not significantly different; numbers with different superscripts are significantly different (chi-square test, $p < 0.005$).

hibit both pol I and pol II activities, actinomycin D (0.5–2 μg/ml [28]) was simply added to the culture medium together with α-amanitin, and embryos were microinjected and processed as above.

Immunofluorescent detection of incorporated BrUTP was performed on fixed specimens as previously described [27]. Incubation with the primary antibody (a mouse monoclonal antibody [IgG] raised against 5-bromo-2′-desoxyuridine (BrdU) and recognizing BrU as well; Caltag Laboratories, Burlingame, CA) diluted 1:500 in PBS + 2% BSA was performed overnight at 4°C. The secondary antibody was a fluorescein isothiocyanate (FITC)-conjugated goat anti-mouse IgG (heavy and light chains, H+L; Jackson ImmunoResearch, West Grove, PA) diluted 1:400 in PBS + 2% BSA. Oocytes were deposited on a slide, mounted in Citifluor (Citifluor Products, Canterbury, England), covered with coverslips, and examined with a Zeiss (Carl Zeiss, Thornwood, NY) inverted microscope after excitation of the FITC at 470 nm. Images were recorded through a charge-coupled device camera (Photometrics, Tucson, AZ; type KAF 1400, 12-bit dynamic range), cooled to 10°C, and coupled to the IPLAB Spectrum Imaging software (Vysis, France). They were stored in a computer for further colocalization analysis. Using a filter wheel for the excitation light and a triple-band dichroic mirror and filter set for emitted light, images from double fluorescent beads taken at two different wavelengths differed at most by a translation of 1 pixel.

Electron Microscopy

SN and NSN oocytes, treated with α-amanitin and injected with BrUTP as described above, were cultured for 30 min and then fixed during 1 h at 4°C in 0.1 M Sörensen buffer (phosphate buffer) containing 2% PFA and 0.2% glutaraldehyde (Sigma). They were then washed three times, 10 min each, in 0.075 M Sörensen buffer, pH 7.2. After blocking of free aldehyde groups in 0.12% glycine in PBS for 15 min, oocytes were washed three times for 5 min each in Sörensen buffer and dehydrated in ethanol series. All these manipulations were done at room temperature. Oocytes were then embedded in LR White (Sigma), and blocks were polymerized at 58°C. Noninjected α-amanitin-treated oocytes were used as controls.

Reactions with antibodies were performed on sections deposited on Formvar (Agar Scientific, Stansted, England)-covered nickel grids. Grids were first floated on normal goat serum (Jackson ImmunoResearch; 1:100 in PBS) for 3 min; they were then incubated overnight at 4°C with the mouse monoclonal anti-BrdU (Caltag Laboratories; 1:20 in PBS containing 2% BSA and 0.025% Tween 20). After thorough rinsing in PBS containing 0.025% Tween 20, they were floated for 3 min in normal goat serum (1:100 in PBS) and incubated for 1 h at room temperature in a goat anti-mouse IgG (H+L) conjugated with 10-nm gold particles (Tebu, Le Perray-en-Yvelines, France; 1:10 in PBS). Grids were then thoroughly washed, first with PBS and then with water, and contrasted by 15-min passage in saturated water-uranyl acetate solution. Control reactions were performed as described above except that the primary antibody was omitted.

Some SN and NSN oocytes were fixed classically as previously described [7] for purely ultrastructural analysis.

RESULTS

In Vivo Changes in the SN:NSN Ratio of Ovarian Oocytes with Age and Hormonal Cycle of the Mice

When analyzing carefully the appearance of the first SN type in oocytes isolated from ovaries of nonstimulated juvenile C57/CBA mice, we found all GV oocytes of NSN or pNSN configuration before 15 days after birth. Beginning from that age, we could collect some GV oocytes with a partial rim of condensed chromatin (pSN) around the nucleolus at 15 and 16 days after birth (Table 1). The first oocytes with a complete rim of perinucleolar chromatin (SN configuration) were obtained from ovaries at Day 17 after birth (10%, n = 139), and their proportion increased rapidly between Days 17 and 18 after birth.

We then analyzed in detail the time dependence of the SN:NSN ratio of large ovarian GV oocytes after hCG-induced ovulation in adult mice. For that purpose, groups of younger (28 days old, i.e., at the beginning of sexual maturity) or older (6 to 8 wk old) mice were synchronized through hCG injection. Several mice were then killed at every time point until 61 h phCG, and the SN:NSN ratio (R) was calculated for oocytes with a diameter of at least 70 μm. Results reported in Figure 1 and Table 2 show that at 13 h after hCG injection, the SN-type oocytes population was very low (R = 0.38) and that it increased progressively during the subsequent hours, although more slowly between 44 and 60 h phCG. As shown in the figure, R measured shortly after ovulation was quite similar for all mice. Later on, R seemed to reach a plateau of around 1 for 6- to 8-wk-old mice, while apparently continuing to increase up to approximately 1.6 at 61 h phCG in 28-day-old mice. Note, however, that the WMW test is not applicable when the samples contain only two elements each, so that the significance of the apparent difference in R values at 60, 61, and 66 h phCG cannot be assessed. At all time points, the main diameter of NSN oocytes was 8–10.5% less than the main diameter of SN oocytes, the difference being always significant (chi test, $p < 0.005$; data not shown).

To further confirm that folliculotropic environment contributes to the enhancement of the SN population, we compared the proportion of SN-type oocytes at 48 h phCG in adult mice stimulated or not with eCG 24 h after hCG induction. We indeed found a significant increase in the proportion of SN-type oocytes (R = 2, n = 98, 2 mice) when

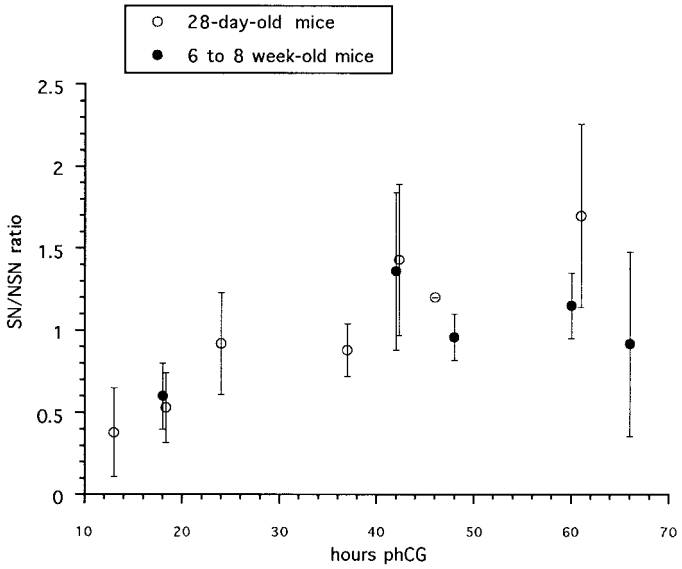

FIG. 1. Variation of the SN:NSN ratio (R) in ovarian GV oocytes with time after hCG injection. R value was measured independently for each mouse killed at the same time. The mean R value and SD at this time are plotted for 28-day-old and 6- to 8-wk-old mice.

the ovary was subjected to the folliculotropic influence provided by eCG as compared to that in controls receiving only hCG (R = 1, n = 115, 3 mice) (chi test, $p < 0.005$).

Correlation between Chromatin Configuration and Transcriptional Activity in Oocytes of Adult and Juvenile Mice

In the search for functional differences between the SN and NSN configurations, we decided to analyze their endogenous pol I- and pol II-dependent RNA synthesis activity through the immunofluorescent detection of BrU incorporated into nascent RNA. GV oocytes isolated from adults (4–9 wk) were classified, either before microinjection (live oocytes) or after immunolabeling (fixed oocytes), in NSN+pNSN and SN+pSN, respectively. After a 10- to 30-min culture following BrUTP microinjection, 94% (n = 117) of NSN+pNSN oocytes showed an intense nuclear fluorescent signal (Fig. 2, A and B; Table 3), while 97% (n = 125) of the SN+pSN oocytes showed no detectable incorporation of BrU, indicating that they were transcriptionally inactive (Fig. 2, C and D, Table 3). In NSN- or pNSN-type oocytes, the fluorescent BrU labeling extended all over

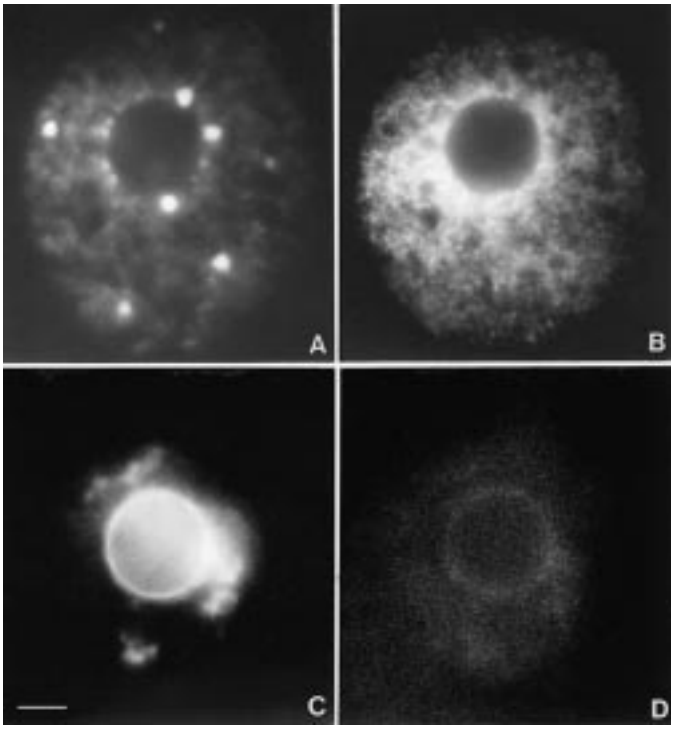

FIG. 2. Detection of transcription in a pNSN (**A, B**) and an SN (**C, D**) GV oocyte. **A, C**) Hoechst staining; **B, D**) immunofluorescent detection of BrU incorporated into nascent RNA after microinjection of BrUTP and incubation for 15–30 min. The gain of the camera and acquisition time were identical in **B** and **D,** allowing a direct comparison between the two images. Oocytes are somewhat squashed between slide and coverslip, so that the NLB is easily distinguishable and the nucleus slightly larger than when oocytes are observed in toto. Note the total absence of transcription in the NLB interior. Bar = 5 μm.

the nucleoplasm, outside the NLB (Fig. 2B). The labeling was not uniform and was mainly located in regions of low or very low Hoechst staining, i.e., decondensed chromatin. Small elongated threads could often be seen arranged along the same line. Increase of the gain of the camera made visible a very faint Hoechst staining behind these threads (Fig. 3, A and B). In contrast, highly fluorescent heterochromatin spots were never stained (Fig. 3, A and B).

The first GV oocytes with the pSN configuration were observed at 15 days, and the first SN oocytes at 17 days after birth, i.e., before sexual maturity. We therefore questioned whether the correlation between chromatin configuration and transcriptional activity holds also at that age.

TABLE 2. Evolution of the R value (SN:NSN) in 28-day-old and 6- to 8-week-old mice.

Age of mice	Hours phCG	No. of mice	Total no. oocytes	Mean R values (± SD)
	13–13.25	3	130	0.38 ± 0.27[a]
	18–18.5	4	172	0.53 ± 0.21[a]
	23.5–24.25	5	191	0.92 ± 0.31[b]
28 Days	36.5–37	2	98	0.88 ± 0.16[b]
	42–42.5	3	88	1.43 ± 0.46[c]
	46	1	24	1.2 (n.d.)*
	61	2	90	1.7 ± 0.56[c]
	18–18.5	4	118	0.6 ± 0.2[a]
	42–42.5	3	102	1.36 ± 0.48[c]
	48	2	118	0.96 ± 0.14[c]
	60	2	76	1.15 ± 0.2[c]
6–8 Weeks	66	2	109	0.92 ± 0.56[c]

* n.d., Not determined.

[a–c] R values with the same superscript letter are not significantly different according to the WMW test; R values with different superscript letters are significantly different (WMW test, α between 0.036 and 0.071).

TABLE 3. Pol II- and pol I-dependent transcriptional activity in GV oocytes of adult and juvenile mice expressed as the percentage of oocytes incorporating BrUTP in the absence (pol I+pol II) or presence (pol I) of α-amanitin.*

	NSN+pNSN		SN+pSN	
Age of mice	−α-amanitin	+α-amanitin	−α-amanitin	+α-amanitin
4–9 Weeks	94% (110/117)[a]	97% (58/60)[a]	3% (4/125)[b]	0% (0/48)
15 Days	82% (28/34)[a]	(−)	(−)	(−)
17 Days	100% (20/20)	(−)	5% (1/21)[b]	(−)
18 Days	(−)	83% (34/41)[a]	(−)	12.5% (2/16)[b]
25 Days	100% (16/16)	100% (5/5)	0% (0/11)	0% (0/5)

* Within parentheses, the denominator is the number of oocytes examined.
[a] Not significantly different from 100% (chi test).
[b] Not significantly different from 0% (chi test).

Indeed, when analyzing RNA synthesis in oocytes of juvenile mice through the incorporation of BrU, we found results identical to those in oocytes of adult mice: all oocytes from 15-day-old mice were of the NSN type and 82% of them were transcriptionally active (n = 34; Table 3). The same was true for NSN oocytes of 17- to 25-day-old mice, while most of the SN oocytes analyzed at Day 17 (95%, n = 21) and 25 (100%, n = 11) failed to show any incorporation of BrU into RNA (Table 3).

In several experiments, we found a small percentage of NSN- or pNSN-type oocytes showing no fluorescent signal. These could have originated from failures of microinjection or from physiological defects of the oocytes. Alternatively, they could represent oocytes that were poorly classified or were just at the limit between activity and inactivity. This holds also for the small percentage of SN- or pSN-type oocytes showing a fluorescent signal.

Transcription of Ribosomal Genes in GV Oocytes

We then addressed the question of the activity and nuclear location of ribosomal genes in fully grown mouse oocytes. To specifically target rRNA synthesis, we used α-amanitin at a concentration (10 μg/ml) known to inhibit pol II-dependent transcription without effect on pol I activity. Under these conditions, the nucleoplasmic transcription signal of NSN- and pNSN-type oocytes was almost completely abolished, except for 8–10 large labeled foci, all located at the outline of the NLB (Fig. 4, A and B). These foci were often ring-shaped and were occasionally prolonged by threads extending to the nucleoplasm. When present (pNSN configuration), perinucleolar condensed heterochromatin foci were not labeled but were next to a transcription site. When two NLBs were present, labeling was observed at the surface of both of them (not shown). Labeling of NSN- and pNSN-type oocytes was completely abolished by actinomycin D addition (0.5–2 μg/ml) to the culture medium before BrUTP microinjection (not shown) and therefore represents pol I-dependent transcription. No labeling was detected in α-amanitin-treated SN and pSN oocytes (Table 3). In some oocytes, individual transcription foci could actually be decomposed as a necklace of smaller intense spots (Fig. 5, A and B) very similar to what has been previously observed in somatic cells [28, 29]. These results clearly show that 1) pol I is active in NSN- and pNSN-type oocytes and 2) ribosomal genes are clustered at the NLB periphery in these oocytes, where they seem to adopt the extended configuration already observed for active ribosomal genes in somatic cells.

As the switch from transcriptional activity to inactivity occurs at some point between NSN and SN configuration, we decided to analyze in more detail the question of what chromatin configuration it corresponds to. For that purpose, we carefully separated, in one experiment with an 18-day-old mouse, NSN from pNSN and SN from pSN oocytes,

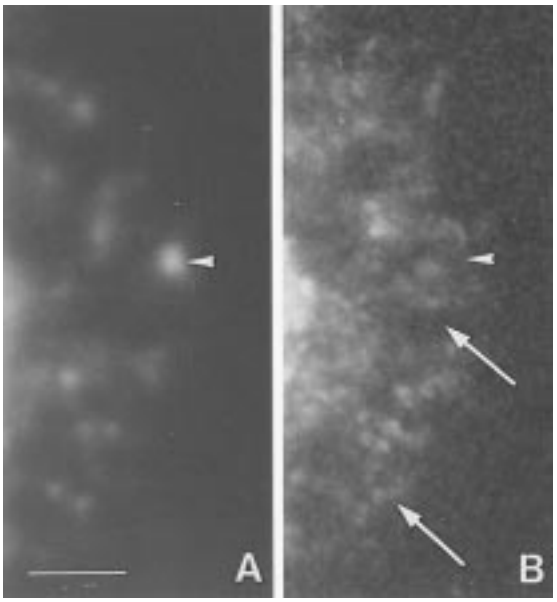

FIG. 3. Expanded image of part of the nucleus of an NSN-type GV oocyte. **A**) Hoechst staining; **B**) immunofluorescent detection of BrU incorporated into nascent RNA. Note that transcription sites extend in areas only faintly labeled with Hoechst (arrows), while highly condensed chromatin is not labeled (arrowhead). Note also the threadlike organization of transcription foci. Bar = 5 μm.

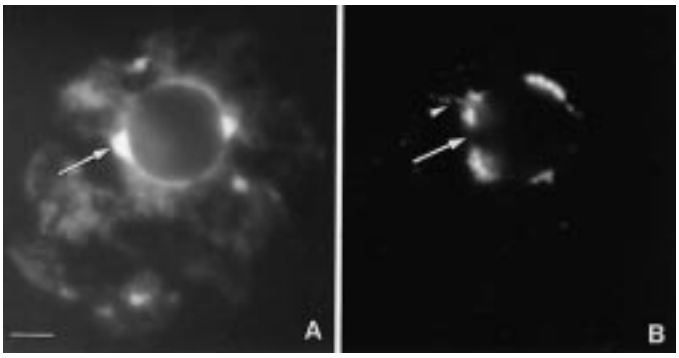

FIG. 4. Transcription of ribosomal genes in an NSN-type oocyte treated by α-amanitin as described in *Materials and Methods.* **A**) Hoechst staining; **B**) immunofluorescent detection of BrU incorporated into nascent RNA, restricted to perinucleolar area. Four discrete foci are visible, with a thread extending into the nucleoplasm (arrowhead). Highly condensed perinucleolar chromatin granules are not labeled but are surrounded by the transcription foci (arrow). Bar = 5 μm.

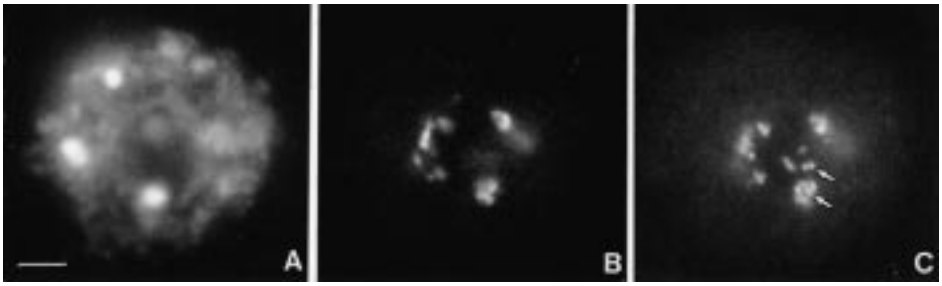

FIG. 5. Ribosomal gene transcription sites in NSN-type GV oocytes can be decomposed into discrete transcription units. **A**) Hoechst staining; **B, C**) nucleolar transcription sites after a short incorporation time (15 min) observed in two different optical planes. Note that each transcription site can be decomposed into a necklace of smaller discrete spots, likely to represent individual transcription units (arrows). Bar = 5 μm.

respectively. We found activity in 83% of the NSN (n = 21) and 83% of the pNSN (n = 18) oocytes, while 80% of pSN (n = 12) and 100% of SN (n = 4) oocytes were inactive. Therefore the transition from transcriptional activity to inactivity seems to occur shortly after the beginning of chromatin wrapping around the NLB.

To analyze whether the discrete pol I transcription sites were associated with special ultrastructural features, we decided to analyze them at the electron microscopy level. For that purpose, some oocytes among those that had been microinjected with BrUTP in the presence of α-amanitin were not processed for immunofluorescence but instead for immunogold detection of incorporated BrU, as indicated in *Materials and Methods.* Several electron microscopy images of nuclei showed a few discrete clusters (usually not more than three per section) of grains at the outer periphery of NLBs (Fig. 6A). These clusters were located in loose and irregular areas of the nucleolar surface, often associated with protrusions of the nucleolar material (Fig. 6A). In some cases, grains were found surrounding small round dense bodies outside the NLBs (Fig. 6B). Vacuoles were not labeled. Microinjected SN oocytes and nonmicroinjected NSN oocytes used as controls showed no labeling (not shown).

To study in more detail the apparent specific ultrastructure of the pol I transcription sites, and to ascertain that loosening of the nucleolar surface and protrusions did not result from the α-amanitin treatment, nonmicroinjected and nontreated oocytes were classically fixed with osmium tetroxide and embedded in Epon (Electron Microscopy Sciences, Ft. Washington, PA) for parallel ultrastructural observation. Despite differences in fixation and embedding procedures, irregularities of the nucleolar surface were indeed observed on some sections of NSN-type oocytes (Fig. 6, C and D), but never in the case of SN-type oocytes (not shown). These irregularities appeared as protrusions of fibrillo-granular material. Comparison of these preparations with specimens processed for immunogold suggests that these peripheral accumulations of fibrillo-granular material do correspond to the pol I transcription sites characterized by accumulation of gold particles.

DISCUSSION

The present work provides new results concerning functional differences associated with the various chromatin configurations found in mouse GV ovarian oocytes of juvenile and adult mice.

We demonstrate a clear-cut correlation between chromatin configuration and transcriptional activity: whatever the age of the mice and the oocyte size, SN- and pSN-type oocytes are silent in relation to pol I- and pol II-dependent transcription, while NSN-type oocytes are actively transcribing. More precisely, the transcriptional activity seems

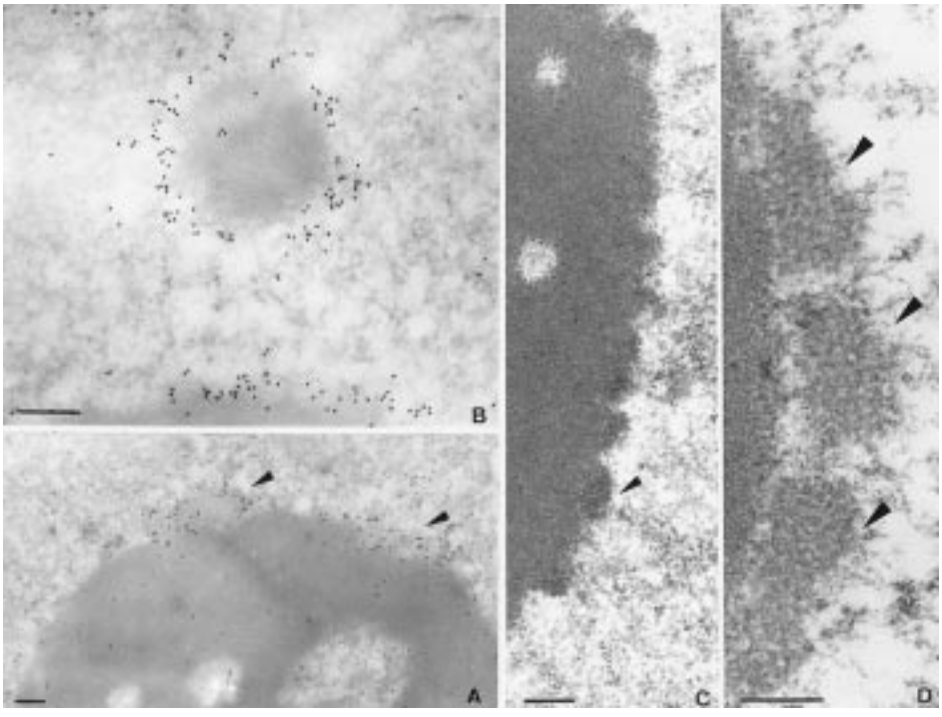

FIG. 6. Ultrastructural localization of sites of rRNA synthesis in NSN-type oocytes. **A, B**) α-Amanitin-treated oocytes microinjected with BrUTP and processed for ultrastructural immunodetection of incorporated BrU as described in *Materials and Methods.* Note the loose structure of the sites of gold particle accumulation (arrowheads). In **B,** gold particles surround a structure detached from the bulk of the NLB. **C, D**) Non-α-amanitin-treated and nonmicroinjected NSN oocytes processed for classical electron microscopy. Despite differences in the fixation and processing of the material, the fibrillo-granular protrusions emanating from the NLB are very comparable to those associated with the transcription sites (arrowheads). Bars = 0.2 μm.

to drop to zero as soon as condensed chromatin begins to wrap around the NLB.

Our results seem then to reconcile several previous studies. Recent studies show a lack of expression of endogenous genes [30] or exogenous DNA templates [31, 32] in the largest oocytes, while older results based on [^{3}H]uridine incorporation were quite contradictory [9, 16–19]. We feel these discrepancies to be due to the size-based classification of oocytes (or follicles), which we show here is not adequate for discriminating active from inactive oocytes. Indeed, NSN oocytes are on average smaller than SN oocytes, but the difference, although significant, is small ([6] and the present study). Therefore discrimination on the criterion of size alone may lead to a mixed NSN/SN population and then to opposite conclusions, depending on the selection conditions. In addition, in cases in which the expression of endogenous or reporter genes has been analyzed [30–32], factors other than transcriptional competence, such as the functionality of the translation machinery or the availability of specific transcription factors, could have interfered with the expression, which is not the case here.

The fact that higher chromatin condensation level and transcriptional inactivity are always associated in SN-type mouse oocytes, irrespective of age of the mice, as well as in human oocytes [15], suggests a biochemical link between these two factors. A likely candidate could be the M phase-specific p34cdc2 kinase, as 1) SN-type GV oocytes present some M-phase characteristics, particularly in terms of microtubule assembly [5]; 2) the acquisition of competence (i.e., the ability of GV oocytes to resume meiotic maturation up to metaphase II, which is higher for SN- than for NSN-type oocytes [5, 6]) is correlated with an increase in p34cdc2 kinase [33, 34] and its activator cdc25 [35], with no substantial changes in the quantity or phosphorylation pattern of mitogen-activated protein kinase [36]; and 3) the involvement of p34cdc2 kinase in the mitotic repression of pol II-dependent transcription was recently shown in vitro [37].

When analyzing the nuclear distribution of pol II-dependent transcription sites in NSN oocytes, we found them clearly associated with the more decondensed chromatin. The threadlike appearance of the fluorescent signal suggests that nascent RNA forms branched chains extending laterally from decondensed chromatin fibers (or loops), which can be visualized only after the sensitivity of the camera is increased. It can be noted that the fluorescent images of transcription sites are very similar to those of ribonucleoprotein fibrils obtained by electron microscopy on chromatin spreads [38].

As far as pol I-dependent transcription is concerned, the present results are consistent with our previous ultrastructural finding of vacuoles inside the NLBs of NSN oocytes [6] and of granular material at their periphery [25], which suggested some residual activity. In SN oocytes, these vacuoles and granules are not found. Actually, we show here that newly synthesized rRNA is located within this perinucleolar granular material, which seems progressively extruded as the compact fibrillar component occupies most of the nucleolar central part [25]. In porcine oocytes, it was not possible to conclude a complete cessation of pol I-dependent activity in fully compact NLBs, as [^{3}H]uridine incorporation was observed after long exposure to the precursor, which is postulated to come from newly synthesized mRNA migrating into the compact nucleolus [20–22]. That we are dealing with newly synthesized rRNA transcripts is shown by the facts that 1) the incorporation is very brief (less that 30 min) and 2) labeling is completely abolished by actinomycin D.

The accumulation of the new rRNA transcripts at the NLB(s) periphery of NSN GV oocytes is a strong indication of the perinucleolar location of rDNA genes within the perinucleolar fibrillo-granular component. This agrees with older cytochemical analyses suggesting the presence of basic and possibly acidic proteins [22, 39, 40], but not of DNA, within the compact mass of mouse and rat NLBs. Also, our previous experiments on NSN-type oocytes of younger mice (10 to 15 days old), in which BrUTP was introduced through permeabilization [28], already suggested a perinucleolar location of active rDNA genes.

The number of pol I transcription domains (8–10) fits well with the accepted number of 5 mouse chromosomes bearing rDNA [41, 42]. As in 3 of them rDNA is paracentromeric [41, 42], the heavily stained chromatin granules close to pol I transcription domains may represent centromeric heterochromatin. The necklace of smaller spots observed within individual transcription sites is likely to represent individual transcription units [43], showing that even in that context of rather condensed prophasic chromatin, ribosomal genes can adopt the extended configuration typical of α-amanitin-treated interphasic somatic cells [44]. In any case, the present results suggest that ribosomal genes remain apposed to the NLB as perinucleolar chromatin progressively wraps around it up to the final SN configuration. Experiments are now under way to analyze more carefully the dynamics of rDNA genes and ribosomal components during oocyte growth and the NSN-to-SN transition, as well as the biochemical factors involved in these dynamics.

Our finding of the first SN configurations in 17-day-old mice correlates well with previous results [5, 7] and confirms that both NSN and SN organizations can coexist when antrum development is initiated. We confirm also that the folliculotropic environment, either naturally occurring during antrum growth or artificially provided by hormonal stimulation of young and adult mice, contributes to turning the NSN organization into SN. The time-dependent variation of R that we observe after hCG-induced ovulation suggests similar hormonal cycle-dependent variations—ovulation preferentially canceling SN oocytes, which would then be progressively restored. However, obviously not all SN oocytes are ovulated. As transcriptionally silent SN oocytes are found as soon as 17 days after birth, the SN population of a given adult mouse includes oocytes that have been stopped in transcription since different time points and may therefore have different RNA (and/or protein) composition. This could provide the biochemical basis for the heterogeneity in the SN capacity to be ovulated and, as elegantly shown recently, to sustain embryonic development [10]. Alternatively, a prolonged blockade of transcription may also be deleterious and lead to atresia.

In conclusion, the demonstration of differential transcriptional activity in NSN versus SN oocytes reconciles previous contradictory results and may represent the biochemical basis of their differential developmental capacities. More analyses are now needed for an understanding of the mechanism of transcriptional arrest and the way in which it is linked to a preovulatory stage in fully grown oocytes. We believe that similar differences could exist among large GV oocytes of other mammalian species and that this diversity could be the basis for different capacities for development after in vitro maturation/in vitro fertilization.

ACKNOWLEDGMENTS

This work is dedicated to Dan Szöllösi, whose brilliant intelligence and original ideas stimulated so many studies, including this one. We thank Stephane Fourgeaud for excellent photographic work and Isabelle Hue for careful reading of the manuscript. We acknowledge the skillful technical assistance of Martine Chebrout.

REFERENCES

1. Sorensen RA, Wassarman P. Relationship between growth and meiotic maturation of the mouse oocyte. Dev Biol 1976; 50:531–536.
2. de Smedt V, Crozet N, Gall L. Morphological and functional changes accompanying the acquisition of meiotic competence in ovarian goat oocytes. J Exp Zool 1994; 269:128–139.
3. Fair T, Hyttel P, Greve T. Bovine oocyte diameter in relation to maturational competence and transcriptional activity. Mol Reprod Dev 1995; 42:437–442.
4. Mattson BA, Albertini DF. Oogenesis: chromatin and microtubule dynamics during meiotic prophase. Mol Reprod Dev 1990; 25:374–383.
5. Wickramasinghe D, Ebert KM, Albertini DF. Meiotic competence acquisition is associated with the appearance of M-phase characteristics in growing mouse oocytes. Dev Biol 1991; 143:162–172.
6. Debey P, Szöllösi MS, Szöllösi D, Vautier D, Girousse A, Besombes D. Competent mouse oocytes isolated from antral follicles exhibit different chromatin organization and follow different maturation dynamics. Mol Reprod Dev 1993; 36:59–74.
7. Zuccotti M, Piccinelli A, Rossi PG, Garagna S, Redi CA. Chromatin organization during mouse oocyte growth. Mol Reprod Dev 1995; 41: 479–485.
8. Tesarik J, Kopecny V, Kurilo LF. Pre-ovulatory RNA synthesis in human oocytes of large antral follicles. Histochem J 1984; 16:438–440.
9. Kopecny V, Landa V, Pavlok A. Localization of nucleic acids in the nucleoli of oocytes and early embryos of mouse and hamster: an autoradiographic study. Mol Reprod Dev 1995; 41:449–458.
10. Zucotti M, Rossi PG, Martinez A, Garagna S, Forabosco A, Redi CA. Meiotic and developmental competence of mouse antral oocytes. Biol Reprod 1998; 58:700–704.
11. Mandl AM. Pre-ovulatory changes in the oocyte of the adult rat. Proc R Soc Lond B Biol Sci 1962; 158:105–118.
12. Crozet N, Motlik J, Szöllösi D. Nucleolar fine structure and RNA synthesis in porcine oocytes during the early stages of antrum formation. Biol Cell 1981; 41:35–42.
13. Lefèvre B, Gougeon A, Nomé F, Testart J. In vivo changes in oocyte germinal vesicle related to follicular quality and size at mid-follicular phase during stimulated cycles in the Cynomolgus monkey. Reprod Nutr Dev 1989; 29:523–532.
14. Tesarik J, Travnic P, Kopecny V, Kristek F. Nucleolar transformations in the human oocyte after completion of growth. Gamete Res 1983; 8:267–277.
15. Parfenov V, Potchukalina G, Dudina L, Kostyuchek D, Gruzova M. Human antral follicles: oocyte nucleus and the karyosphere formation (electron microscopic and autoradiographic data). Gamete Res 1989; 22:219–231.
16. Moore GPM, Lintern-Moore S, Peters H, Faber M. RNA synthesis in the mouse oocyte. J Cell Biol 1974; 60:416–422.
17. Wassarman PM, Letourneau GE. RNA synthesis in fully-grown mouse oocytes. Nature 1976; 261:73–74.
18. Bloom AM, Mukherjee BB. RNA synthesis in maturing mouse oocytes. Exp Cell Res 1972; 74:577–582.
19. Rodman TC, Bachvarova R. RNA synthesis in preovulatory mouse oocytes. J Cell Biol 1976; 70:251–257.
20. Crozet N, Kanka J, Motlik J, Fulka J. Nucleolar fine structure and RNA synthesis in bovine oocytes from antral follicles. Gamete Res 1986; 14:65–73.
21. Motlik J, Fulka J. Factors affecting meiotic competence in pig oocytes. Theriogenology 1986; 25:87–96.
22. Crozet N. Nucleolar structure and RNA synthesis in mammalian oocytes. J Reprod Fertil 1989; 38:9–16.
23. Tesarik J, Kopecny V, Dvorak M, Pilka L, Kurilo LF. Human nonovulatory oocyte-cumulus complexes: ultrastructure, macromolecular synthesis, and development potential. Gamete Res 1984; 9:153–165.
24. Vautier D, Besombes D, Chassoux D, Aubry F, Debey P. Redistribution of nuclear antigens linked to cell proliferation and RNA processing in mouse oocytes and early embryos. Mol Reprod Dev 1994; 38: 119–130.
25. Borsuk E, Vautier D, Szöllösi MS, Besombes D, Debey P. Development-dependent localization of nuclear antigens in growing mouse oocytes. Mol Reprod Dev 1996; 43:376–386.
26. Wansink DG, Schul W, van der Kraan I, van Steensel B, van Driel R, de Jong L. Fluorescent labeling of nascent RNA reveals transcription by RNA polymerase II in domains scattered throughout the nucleus. J Cell Biol 1993; 122:283–293.
27. Bouniol C, Nguyen E, Debey P. Endogenous transcription occurs at the 1-cell stage in the mouse embryo. Exp Cell Res 1995; 218:57–62.
28. Masson C, Bouniol C, Fomproix N, Szöllösi MS, Debey P, Hernandez-Verdun D. Conditions favoring RNA polymerase I transcription in permeabilized cells. Exp Cell Res 1996; 226:114–125.
29. Junera HR, Masson C, Géraud G, Suja J, Hernandez-Verdun D. Involvement of in situ conformation of ribosomal genes and selective distribution of upstream binding factor in rRNA transcription. Mol Biol Cell 1997; 8:145–156.
30. Curci A, Bevilacqua A, Fiorenza MT, Mangia F. Developmental regulation of heat-shock response in mouse oogenesis: identification of differentially responsive oocyte classes during graafian follicle development. Dev Biol 1991; 144:362–368.
31. Bevilacqua A, Kinnunen LH, Mangia F. Genetic manipulation of mammalian dictyate oocytes: factors affecting transient expression of microinjected DNA templates. Mol Reprod Dev 1992; 33:124–130.
32. Worrad DM, Ram PT, Schultz RM. Regulation of gene expression in the mouse oocyte and early preimplantation embryo: developmental changes in Sp1 and TATA box-binding protein, TBP. Development 1994; 120:2347–2357.
33. de Vantéry C, Gavin AC, Vassalli JD, Schorderet-Slatikine S. An accumulation of p34cdc2 at the end of mouse oocyte growth correlates with the acquisition of meiotic competence. Dev Biol 1996; 174:335–344.
34. Chesnel F, Eppig JJ. Synthesis and accumulation of p34cdc2 and cyclin B1 in mouse oocytes during acquisition of competence to resume meiosis. Mol Reprod Dev 1995; 40:503–608.
35. Mitra J, Schultz RM. Regulation of the acquisition of meiotic competence in the mouse: changes in the subcellular localization of cdc2, cyclin B1, cdc25C and wee1, and in the concentration of these proteins and their transcripts. J Cell Sci 1996; 109:2407–2415.
36. Harrouk W, Clarke HJ. Mitogen-activated protein (MAP) kinase during the acquisition of meiotic competence by growing oocytes of the mouse. Mol Reprod Dev 1995; 41:29–36.
37. Leresche A, Wolf VJ, Gottesfeld JM. Repression of RNA polymerase II and III transcription during M phase of the cell cycle. Exp Cell Res 1996; 229:282–288.
38. Bachvarova R, Burns JP, Spiegelman I, Choy J, Chaganti RSK. Morphology and transcriptional activity of mouse oocyte chromosomes. Chromosoma 1982; 86:181–196.
39. Takeuchi IK. Electron microscopic study on the bismuth staining of nucleoli in growing mouse oocytes. Acta Histochem Cytochem 1987; 20:295–304.
40. Antoine N, Lepoint A, Baeckeland E, Goessens G. Ultrastructural cytochemistry of the nucleolus in rat oocytes at the end of the folliculogenesis. Histochemistry 1988; 89:221–226.
41. Geuskens M, Alexandre H. Ultrastructural and autoradiographic studies of nucleolar development and rDNA transcription in preimplantation mouse embryos. Cell Differ 1984; 14:125–134.
42. Elsevier SM, Ruddle FH. Localization of genes coding for 18S and 28 S ribosomal RNA within the genome of *Mus musculus.* Chromosoma 1975; 52:219–228.
43. Haaf T, Hayman DL, Schmid M. Quantitative determination of rDNA transcription units in vertebrate cells. Exp Cell Res 1991; 193:78–86.
44. Haaf T, Ward DC. Inhibition of RNA polymerase II transcription causes chromatin decondensation, loss of nucleolar structure, and dispersion of chromosomal domains. Exp Cell Res 1996; 224:163–173.